Received: 3 October 2021 | Accepted: 11 January 2022 | Published online: 16 February 2022

DOI: 10.1111/opo.12959

OPO THE COLLEGE OF OPTOMETRISTS

ORIGINAL ARTICLE

Modelling the refractive and imaging impact of multi-zone lenses utilised for myopia control in children's eyes

Raman Prasad Sah | **Matt Jaskulski** | **Pete S Kollbaum**

School of Optometry, Indiana University, Bloomington, Indiana, USA

Correspondence
Raman Prasad Sah, School of Optometry, Indiana University, Bloomington, Indiana, USA.
Email: rsah@iu.edu

Funding information
None.

Abstract

Purpose: To develop an optical model of a child's eye to reveal the impact of target distance and accommodative behaviour on retinal image quality when fitted with multi-zone lenses.

Methods: Pupil size, aberration levels and accommodative lag were adjusted for models viewing stimuli at 400, 100, 33 and 20 cm. Distributions of defocus across the pupil and simulated retinal images were obtained. An equivalent 16-point letter was imaged at near viewing distances, while a 0.00 logMAR (6/6) letter was imaged at 400 cm. Multi-zone lenses included those clinically utilised for myopia control (e.g., dual-focus, multi-segmented and aspherical optics).

Results: Viewing distance adjustments to model spherical aberration (SA) and pupil radius resulted in a model eye with wider defocus distributions at closer viewing distances, especially at 20 cm. The increasing negative SA at near reduced the effective add power of dual-focus lenses, reducing the amount of myopic defocus introduced by the centre-distance, 2-zone design. The negative SA at near largely compensated for the high positive SA introduced by the aspheric lens, removing most myopic defocus when viewing at near. A 0.50 D accommodative lag had little impact on the legibility of typical text (16-point) at the closer viewing distances.

Conclusions: All four multi-zone lenses successfully generated myopic defocus at greater viewing distances, but two failed to introduce significant amounts of myopic defocus at the nearest viewing distance due to the combined effects of pupil miosis and negative SA. Typical 16-point type is easily legible at near even in presence of the multi-zone optics of lenses utilised for myopia control and accommodative lag.

KEYWORDS
aberrations, accommodation, defocus, multi-zone lenses, myopia, simulated retinal image

INTRODUCTION

The prevalence of myopia has been steadily increasing in recent years, affecting approximately 33% of the US population,[1] and over 90% of children and young adults in regions of East and Southeast Asia.[2–5] Several optical interventions, including bifocal and progressive addition spectacles,[6] dual and multifocal contact lenses[7,8] and more recently, multi-segmented spectacles[9,10] have been used in an effort to slow myopia progression by introducing myopic defocus into the eyes of progressing myopes.

Multi-zone optics must balance the requirement for high quality vision with the need to introduce myopic defocus (treatment effect). Multi-zone optics have attained high quality distance vision in presbyopic and pseudophakic eyes,[11–13] and similar results are observed in young adults[14–16] and children[8,17,18] fitted with multi-zone lenses. However, because of accommodative lags,[19] shifts of ocular spherical aberration from positive to negative[20] and varying degrees of pupil miosis[21] which may occur with accommodation during near viewing, the optical impact of multi-zone lenses is susceptible to change with viewing distance. Also, some multifocal designs have been shown to reduce accommodation whereas eyes fitted with a dual focus lens showed normal accommodation.[22] Can multi-zone lenses, such as those that are clinically used for myopia control, achieve the joint goals of introducing myopic defocus and retaining high quality vision over the range of viewing distances commonly encountered by children?

The present study used optical modelling to examine systematically the refractive state distribution and image quality in optical models of children's eyes, taking into account accommodative lags, viewing distance dependent changes in pupil sizes and spherical aberration. Optical properties of eyes alone and those fitted with multi-zone lenses were compared.

Key points

- Multi-zone lenses may generate myopic defocus at greater viewing distances yet fail to introduce significant myopic defocus at the nearest viewing distance due to pupil miosis and negative spherical aberration.
- The presence of multi-zone optics does not impair the legibility of typically encountered 16-point type at near.
- Knowledge of a child's accommodative behaviour, spherical aberration and pupil miosis associated with near work may aid optical treatments to slow myopia progression.

METHODS

Model parameters

An optical model of the accommodating child's eye based on its wavefront error (WFE) was developed to examine the impact of changing pupil size, monochromatic aberrations, accommodative error and angular size of viewed stimuli that accompany near viewing. Ex-vivo wavefronts for four different multi-zone lenses measured using a validated, single-pass Shack-Hartmann aberrometer (ClearWave, Lumetrics, lumetrics.com)[23] were added to the modelled children's eyes to assess their refractive and imaging effects.

Viewing distances favoured by children vary with age, height, type of visual task and arm length (Harmon distance),[24] but reading distances are typically between 33 and 20 cm.[25,26] Viewing distances of 400, 100, 33 and 20 cm were included in our model (Table 1). Images of an upper-case, non-serifed letter E were computed for letters subtending 5 arc minutes (0.00 logMAR (6/6) letter) at 400 cm, and for text size typically encountered in children's books,[27] 16-point type (2 M) letters,[28] which subtended 10, 30 and 50 arc minutes at 100, 33 and 20 cm, respectively.

Kirwan et al.[29] reported higher order aberrations (HOA) from 162 unaccommodated eyes of 82 children (ages 4–14) for a 6 mm pupil diameter. Their absolute mean Zernike coefficient (up to 5th order) with signs matching the arithmetic mean were included in our model scaled to the model pupil sizes. Studies of children show that as the eye accommodates, pupil size decreases[21] and spherical aberration becomes increasingly more negative.[30] We used currently unpublished laboratory data obtained from 16 myopic children (aged 8–13 years) viewing 0.30 logMAR (6/12) letter targets over six distances (between 400 and 20 cm) to model the viewing distant dependent spherical aberration and pupil size. Data were collected on right eyes with binocular viewing of the letter targets on an iPhone (Apple, apple.com), using a double pass pyramidal wavefront aberrometer (Osiris, CSO, csoitalia.it). A mixed quadratic model was used to predict spherical aberration (C_4^0) values for natural pupil radii of 3.32, 3.48, 3.47 and 2.81 mm of +0.13, +0.02, −0.17 and −0.26 µm, respectively, for viewing distances of 400, 100, 33 and 20 cm (Table 1). These values represent averages observed when children viewed stimuli over target vergences (TV) between −0.25 and −5.00 D with natural pupils. Actual accommodation levels varied slightly between eyes due to varying levels of accommodative lag, and we have employed the average observed SA levels for both the accurate and lagging eyes as representative of average SA experienced by children at these TV. Image quality is affected by even small amounts of defocus. Defocus due to accommodative lag is common, and has been reported either to be less than 0.50 D[31,32] or reach up to 2.00 D in myopic children.[19] However, 0.50 D of lag is typical for children

TABLE 1 Model parameters used for an accommodating child's eye

Viewing distances	400 cm	100 cm	33 cm	20 cm
Pupil radii	3.32 mm	3.48 mm	3.47 mm	2.81 mm
Spherical aberration	+0.13 μm	+0.02 μm	−0.17 μm	−0.26 μm

A mixed quadratic model was applied to our laboratory's previously collected data in children ($n = 16$) to predict natural pupil sizes and spherical aberration for corresponding viewing distances.

viewing near targets.[19] Thus, we compared images for optimally focused model eyes (details explained in Data Analysis) with the same models experiencing 0.50 D of typically encountered accommodative lag.

Four commercially available multi-zone lenses (three contact lenses and one spectacle lens) were included in the model: MiSight 1 day (CooperVision, coopervision.com); Biofinity Multifocal centre-distance (CD) (CooperVision, coopervision.com); NaturalVue Multifocal 1 Day (Visioneering Technologies, vtivision.com) contact lenses and Defocus Incorporated Multiple Segments (DIMS) spectacle lenses, currently marketed as MiYOSMART[33] (Hoya Vision, hoyavision.com) (Figure 1), all of which have been either employed (on- or off-label) or investigated as potential myopia control interventions.[7,8,10,18,34] MiSight 1 day is a dual-focus contact lens approved by the US Food and Drug Administration (FDA) for controlling myopia progression in children.[35] Biofinity Multifocal CD and NaturalVue Multifocal 1 Day are contact lenses designed for the treatment of presbyopia, but are also clinically used off-label for myopia control.[7,34] DIMS is a dual-focus spectacle lens designed for myopia control in children.[10,18,33] ClearWave-measured wavefronts from each lens were individually added to the modelled child's eye wavefront in the pupil plane using proprietary analysis software - Indiana Wavefront Analyzer (IWA) written in MATLAB (MathWorks, mathworks.com). Contact lens models assumed complete contact lens conformation.[14,36]

Data analysis

As some multi-zone lenses contain distance viewing optics centrally, and others near viewing optics centrally, this requires careful determination of optimal focus as entered into the model. Optimum focus for the "eye alone" model and "eye + lens" model corresponding to the aspheric NaturalVue Multifocal 1 Day lens was determined by identifying the over-correction that maximized the visual Strehl ratio based on the optical transfer function (VSOTF) image quality metric.[37] For comparison, three additional focus strategies were employed. One that minimized wavefront root mean square error (RMSE), i.e.,:

$$\text{minRMS refractive state } (D) = (-4.\sqrt{3}.C_2^0)/R^2 \quad (1)$$

Two additional refractive states were considered. One that focused the eye paraxially, where

$$\text{Paraxial refractive state } (D) = (-4.\sqrt{3}.C_2^0 + 12.\sqrt{5}.C_4^0)/R^2 \quad (2)$$

and one that focused the pupil margins:

$$\text{Marginal refractive state } (D) = (-4.\sqrt{3}.C_2^0 - 12.\sqrt{5}.C_4^0)/R^2 \quad (3)$$

where R is pupil radius in mm and C_n^m are the Zernike coefficients of the measured wavefront in micrometres.[38]

For the two other contact lenses (MiSight 1 day and Biofinity Multifocal CD), the "eye + lens" models were focused by setting the mean defocus of either the centre zone (distance zone focus) or the first annular zone (treatment/add zone focus) to zero by adding appropriate C_2^0 to the model. For treatment/add zone focus, there is no accommodative behaviour that would allow the add zone to be focused at target vergences more distant than the add power of the lens; hence, only the results from the two nearer target vergences (TV = −3.00 and −5.00 D) are shown. For an eye viewing through the peripheral optics of the DIMS spectacle lens, the distance optic was focused (minRMS).

In an optimally focused eye with aberrations, and even more so in the same eye wearing a multi-zone lens, there can be a wide range of refractive states at different locations in the pupil.[39] Using either the "(wavefront slope)/r" calculation for sagittal refractive state or a refractive state calculated from local curvature,[40] we computed local refractive state at each pupil sampling point, and from these refractive state maps we computed the distributions of defocus present in the modelled child's eye, taking into account the Stiles-Crawford effect and diminishing the efficacy of light rays further away from the pupil centre[41,42] using the equation:

$$\text{Defocus} = \text{refractive state (RS)} - \text{target vergence (TV)} \quad (4)$$

Following Equation (4), myopic defocus is accompanied by a negative sign and hyperopic defocus by a positive sign. The defocus distributions quantify the magnitude of the myopic defocus "stop signal", or conversely, the hyperopic "grow signal". The "eye alone" or "eye + lens" WFE maps were used to compute image plane point spread functions (PSF) and corresponding optical transfer functions (OTF). The product of these OTF and the Fourier transform of the visual stimuli were computed to obtain the simulated retinal image by means of an inverse Fourier transform.[43]

RESULTS

Model eye

The majority of the light entering through the pupil of an aberrated eye is to a greater or lesser extent defocused,[39] and due to spherical aberration (SA), the refractive state at

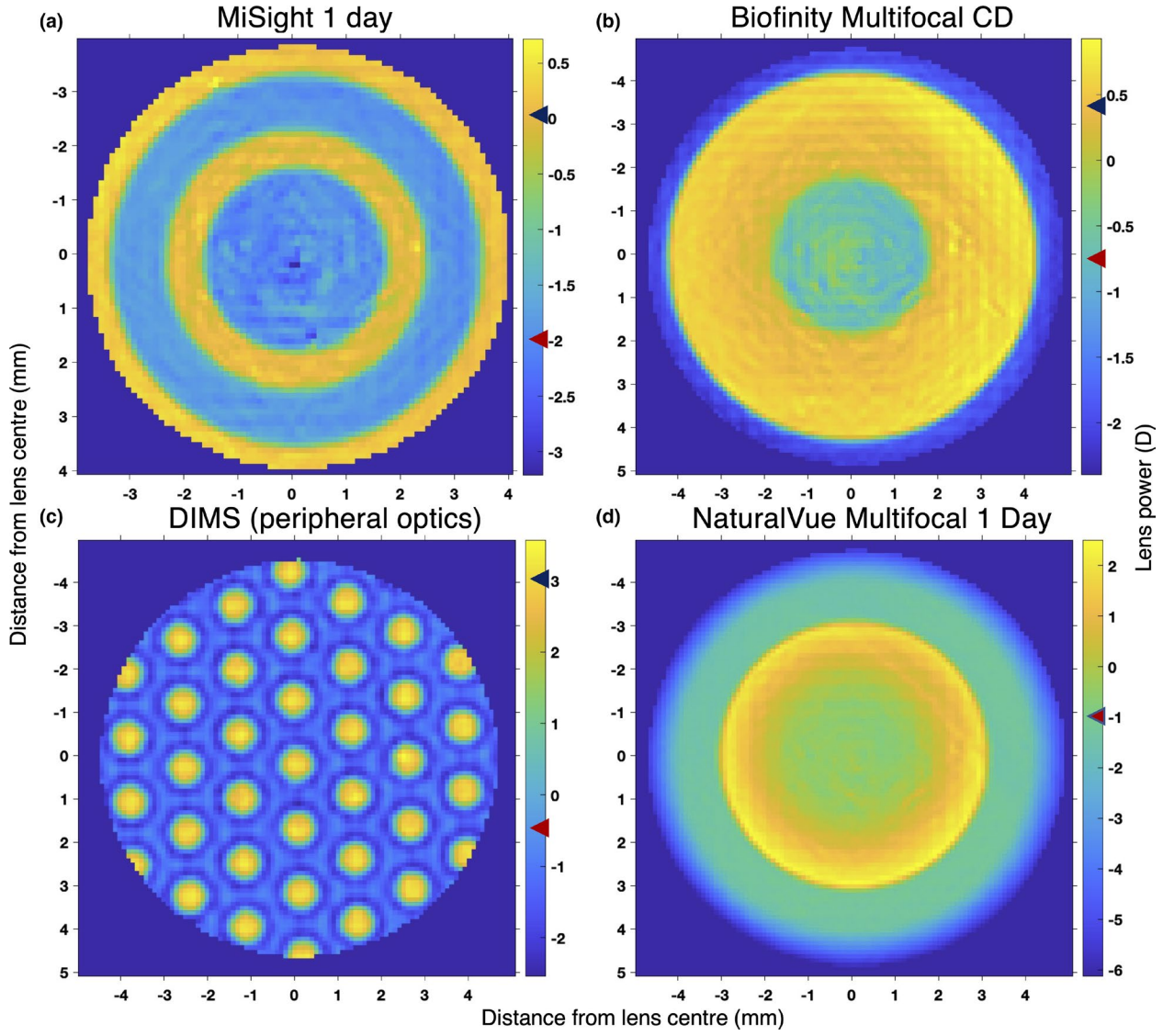

FIGURE 1 Ex-vivo, aberrometer measured power maps of four myopia control lenses. (a), (b) and (d) represent sagittal powers maps for MiSight 1 day, Biofinity Multifocal centre- systematically distance (CD) and NaturalVue Multifocal 1 Day contact lenses, respectively, whereas (c) represents the curvature power map of the peripheral region of a Defocus Incorporated Multiple Segments (DIMS) spectacle lens. The red and blue triangles on the colour bar scale indicates the measured distance and add power, respectively. Note that these measured powers served as the basis for optical modelling as opposed to the nominally labelled powers on the packaging

the pupil centre can differ from that at the pupil margin by more than 2.00 D.[38] Significantly, the defocus created when focusing a specific region of the pupil will vary with viewing distance because SA may change magnitude and sign with accommodation.[20] The interaction between the computational focusing strategy and resulting defocus distributions are compared in Figure 2 for the accommodating model child's eye viewing stimuli at 400, 100, 33 and 20 cm (target vergences of −0.25, −1.00, −3.00 and −5.00 D, respectively). The resulting defocus distributions are similar for children's eyes, accommodating for TV of −0.25, −1.00 and −3.00 D, revealing a peak at or near zero when defocus is adjusted to maximise image quality (Figure 2b, Optimum IQ focus), and the majority of the pupil generates defocus of <0.50 D. Notably, for the model eye accommodating to a 20 cm target, the elevated levels of negative SA cause a much wider spread of the refractive distribution, with 36% of the pupil being defocused by >0.50 D even when optimally focused. Comparison of the optimum focus distributions with paraxial and minRMS focus reveals that optimum focus is achieved by focusing between these two standard choices of focus, as has been reported for adult eyes.[44] In the presence of considerable negative SA, the paraxial focusing strategy generated large amounts of hyperopic defocus, especially for the 20 cm accommodating model, whereas with marginal focus large amounts of myopic defocus were generated. For an eye with positive SA, accommodative lag will tend to focus the pupil margins, whereas with negative SA, accommodative lag will shift focus towards the pupil centre. Marginal and to a lesser extent paraxial focus resulted in significant levels of defocus when SA levels are high (Figure 2c, d).

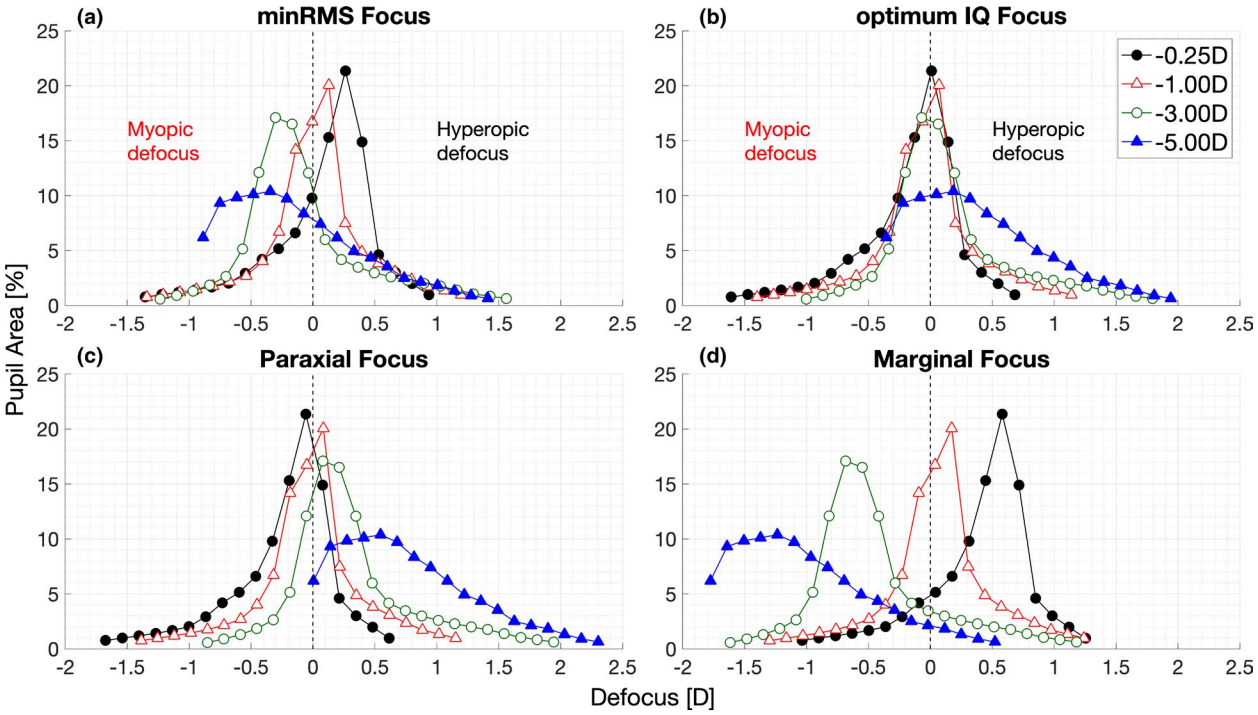

FIGURE 2 Impact of optics of an accommodating model child's eye. Defocus distributions at four target vergences (step size 0.125 D) employing different focusing strategies[37,38] are shown. Defocus equals refractive state minus target vergence

The impact of these four focusing strategies on the accommodating child's eye, either with or without a 0.50 D accommodative lag, is revealed by the PSF and simulated retinal images in Figure 3. In the presence of larger amounts of negative SA, the hyperopic defocus contributed by lag improved IQ in a model otherwise marginally focused, but lags created increased blur when hyperopic defocus dominated, e.g., when added to an otherwise paraxially focused eye. In spite of the varied levels of blur generated by these eight models (four focusing strategies, each with and without the lag), the 16-point type character was easily recognizable when viewed at both near distances (33 and 20 cm) even with the increased defocus (Figure 2) and blur (see PSF, Figure 3) at these near distances.

Note that the letter E at 400 cm subtends 5 min of arc (analogous to 0.0 logMAR) whereas at distances of 100, 33 and 20 cm it subtends 10, 30 and 50 min of arc, respectively; analogous to a child viewing 16-point type at corresponding near viewing distances. All images shown are square plots, PSF ranging from −15 to +15 min of arc, and the simulated retinal image ranging from −35 to +35 min of arc. For 400 and 100 cm viewing distances where the simulated images are small, the background was filled with white. The same conventions apply to the remaining simulation figures.

Model eye + MiSight 1 day lens

The MiSight 1 day dual-focus lens includes a distance correction in the centre zone surrounded by the first annular treatment ring (treatment zone), a second annular distance zone and finally a second annular treatment zone with corresponding diameters of approximately 3.40, 4.80, 6.80 and 8.80 mm, respectively[14] (Figure 1a). The two image planes generated in a non-lagging eye are shown schematically in Figure 4a. The defocus distributions for an "eye + lens" model that has been focused for the centre zone (CZ) distance optic (Figure 4b) revealed a second peak at about −2.00 D (myopic defocus). This is as expected from the +2.00 D added to the treatment zones (Figure 1a) for this lens. The large amount of negative SA in the −5.00 D TV model reduced the effective power within the treatment zone, resulting in the shift of this peak towards less myopic values (between −1.00 and −1.50 D). If a child used the +2.00 D power added in the treatment zones to focus near targets, large amounts of hyperopic defocus would be generated by the central and annular distance zone optics (Figure 4c). However, there is no evidence children[45] or young adults[22] wearing MiSight lens actually use the power in the treatment zones to focus near targets; although, the recent study by Gifford et al. suggests the possibility of a multifocal contact lens design to affect the accommodative behaviour in young adults.[22]

Figure 5 shows the PSF and simulated retinal images revealing the impact of the MiSight 1 day lens on the model eye focusing either the power in the distant or treatment zones. For an eye focusing the distance zones, the PSF was dominated by a well-focused, small central core surrounded by a myopically defocused ring. This myopically defocused ring was centrally enlarged, but surrounded by a smaller myopically defocused ring in the presence of lag,

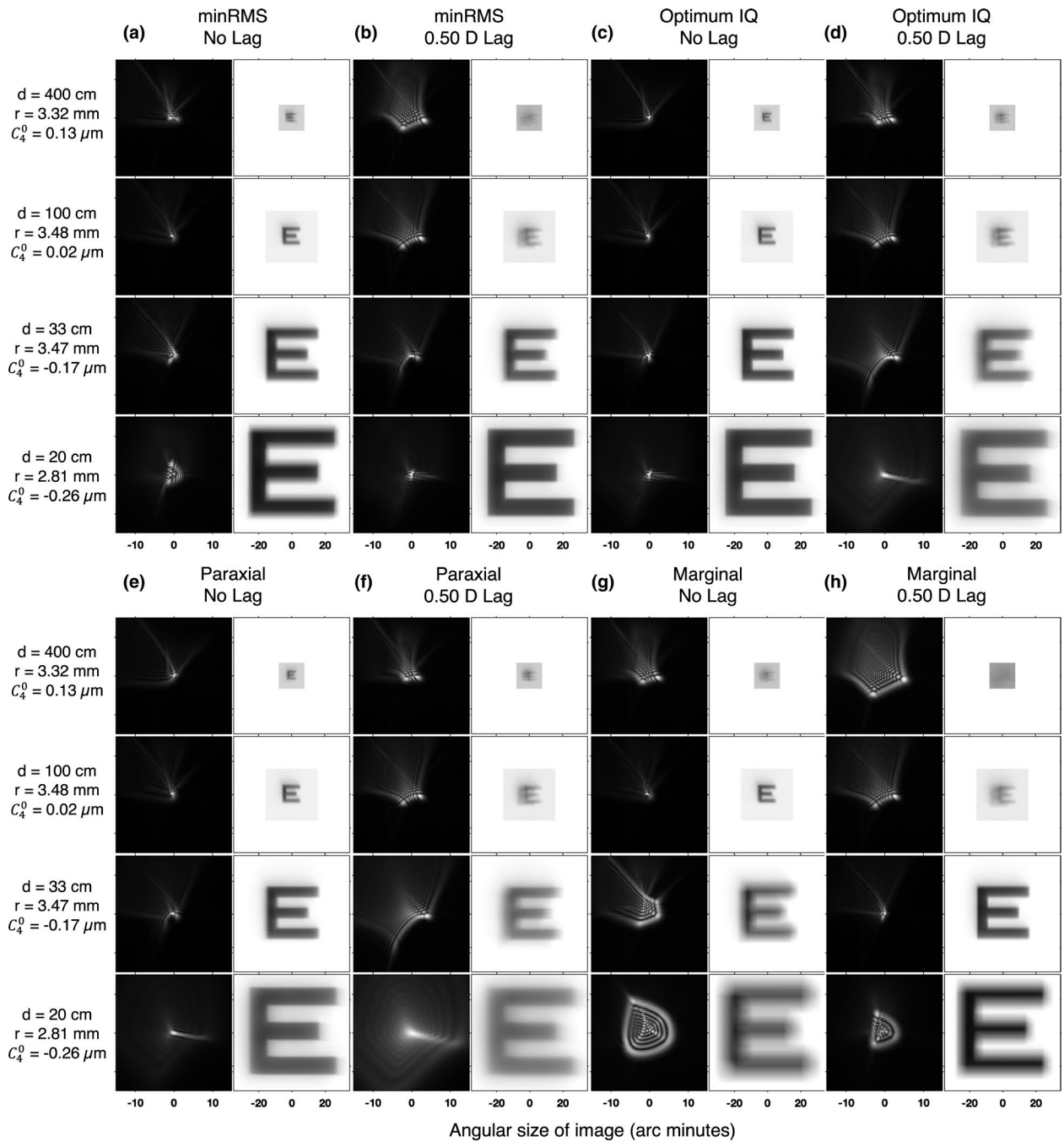

FIGURE 3 Impact of optics of an accommodating model child's eye. Point Spread Functions (PSF) and simulated retinal images of letter E computed for different viewing distances and employing different focusing strategies are shown as mentioned at the top. For each strategy, the effect of typical lag (0.50 D) is shown

reducing the IQ at 400 cm. Similarly, for an eye focusing the treatment zones, the PSF was dominated by an imperfectly focused central core surrounded by a hyperopically defocused patch from the defocused central zone. Also, the negative SA at near (33 and 20 cm) counteracted some of the myopic defocus created by the treatment zones when focusing the distant zone resulting in a decrease in the size of the blur annulus. As is expected from any dual focus lens, the defocused light reduced the contrast of the focused image, but the increased angular size of the image at near viewing distances helped to retain the high legibility of the letter for both distant and treatment zone focus, even in presence of an accommodative lag.

Model eye + Biofinity Multifocal centre-distance (CD) lens

The Biofinity Multifocal CD lens is comprised of a single distance zone in the centre (r = 1.80 mm) surrounded by a

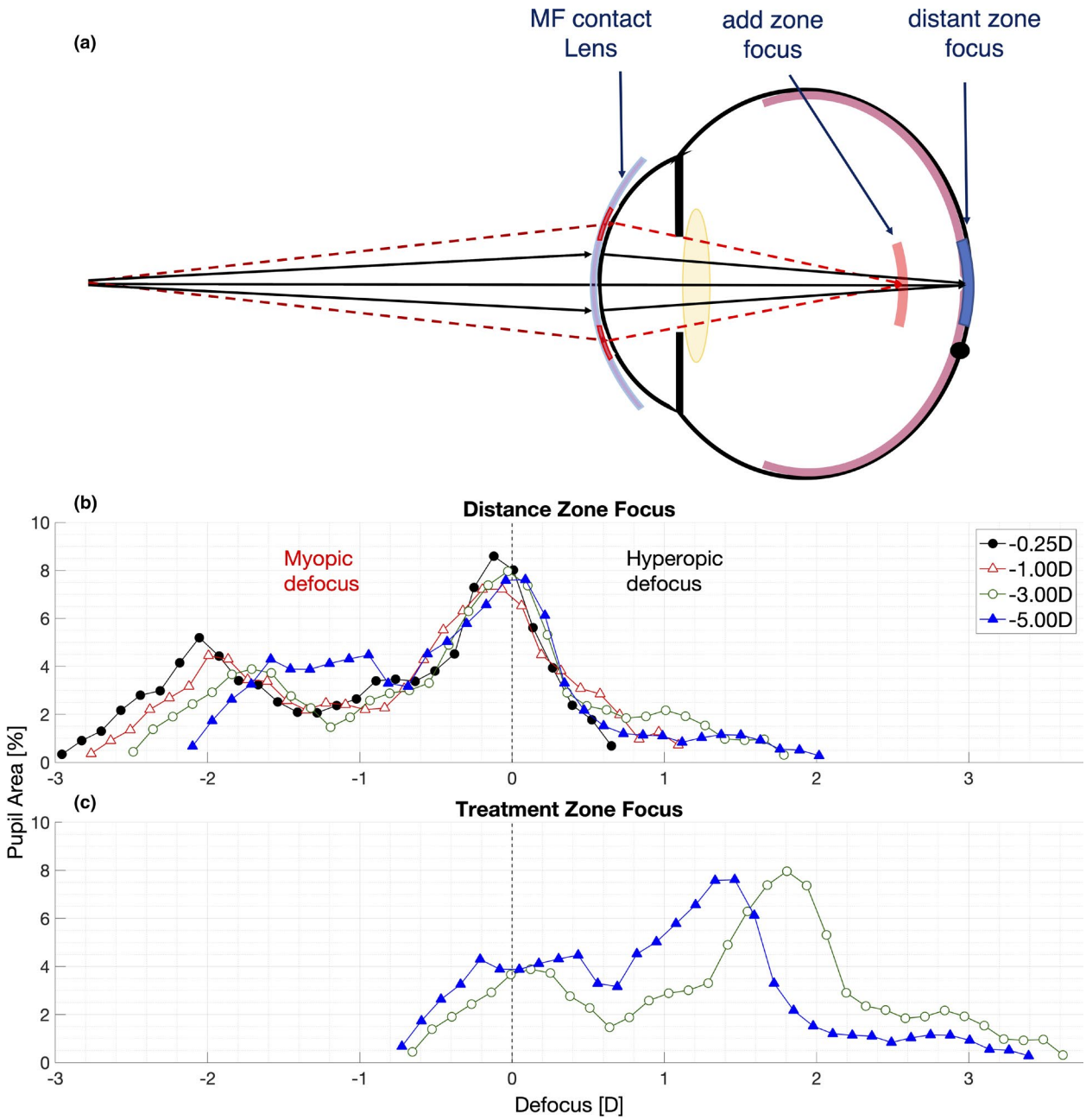

FIGURE 4 Impact of adding a MiSight 1 day contact lens to the accommodating model child's eye. (a) Schematic of a model child's eye wearing a dual-focus contact lens, showing focal planes for the distance correction and add (treatment) zones when viewing a near target. Defocus distributions using (b) distance focus at four different target vergences and (c) treatment zone focus at two near target vergences are shown. For treatment zone focus, the data has shifted by the lens specified +2.00 D of additional power. Defocus equals refractive state minus target vergence

single add zone (Figure 1b). The bi-modal defocus distributions for an eye focusing with the distance zone (Figure 6a) manifested a second peak at around −1.30 D for the −0.25 D TV, which gradually shifted to around −1.21 and −0.88 D for −1.00 and −3.00 D TV, respectively, and was ultimately lost for the −5.0 D TV. The maximum myopic defocus also reduced from around −3.00 D at −0.25 D TV to <−1.00 D at −5.00 D TV due to pupil miosis and the presence of negative SA at near. Alternatively, if an eye used the add zone to focus, (Figure 6b), the majority of the defocus was shifted towards hyperopia. The PSFs and simulated retinal images calculated for the model "eye + lens" (Figure 7) exhibited a well-focused central core surrounded by an aberrated skirt when the distance zone was focused. At the nearest viewing distances (33 and 20 cm), the myopic defocus created by the surrounding add zone was dioptrically reduced due to negative SA, while also reduced its proportion of light because of near pupil miosis. Both of these resulted in significantly improved image contrast at the 20 cm viewing distance.

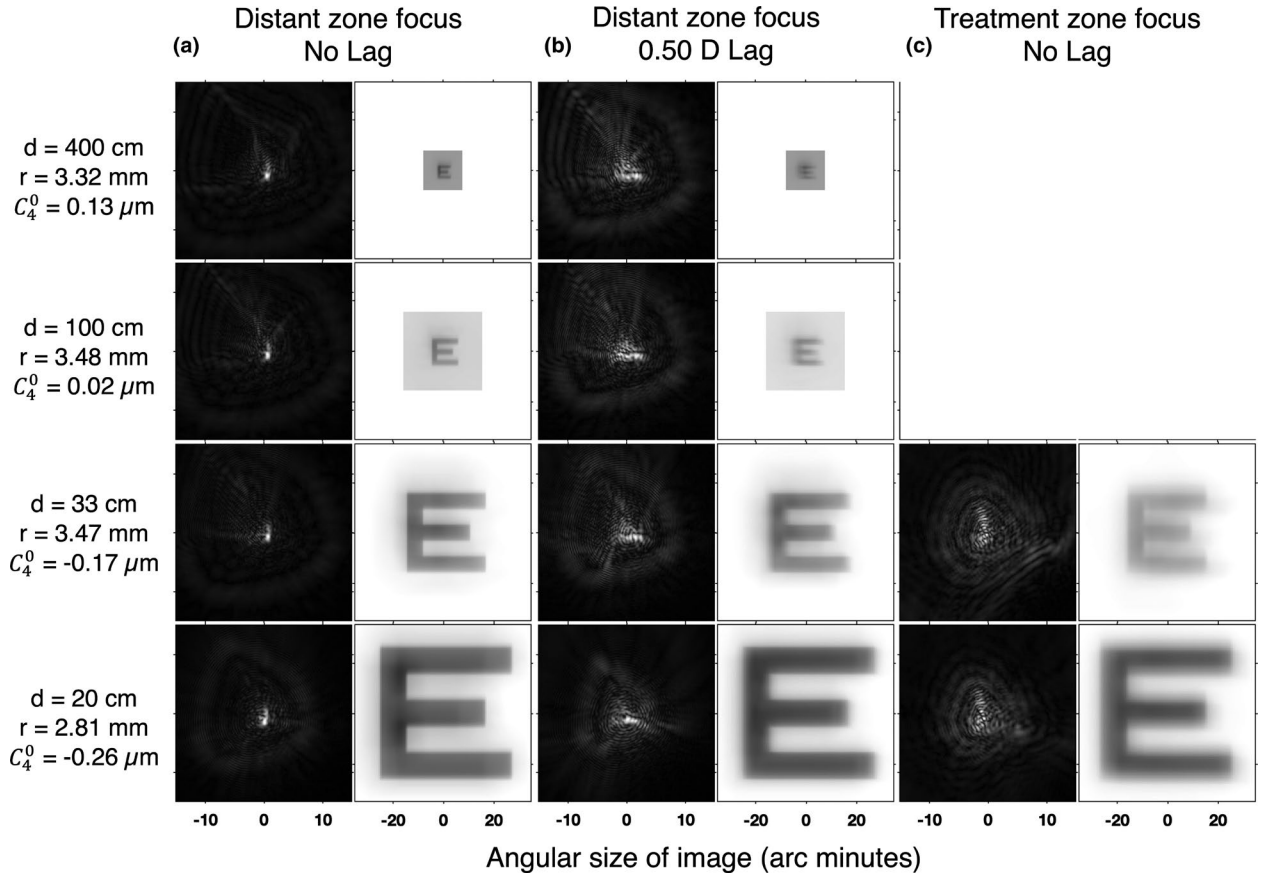

FIGURE 5 Impact of adding MiSight 1 day contact lens to the accommodating model child's eye. Point Spread Functions (PSF) and simulated retinal images of a letter E are computed for different viewing distances for a model eye focusing either the distance zone or treatment zone as mentioned at the top. For distance zone focus, the effect of typical lag (0.50 D) is also shown

Model eye + Defocus Incorporated Multiple Segments (DIMS) lens

The DIMS spectacle lens includes a novel multi-segmented optical design comprising of a central distance optic zone (9 mm in diameter) surrounded by an annular zone including multiple circular lenslets approximately 1 mm in diameter and of relative positive (add) power of +3.50 D (Figure 1c, inset Figure 8).[18,40] The defocus distributions obtained for an eye viewing solely through the central (distance) zone (data not shown) are similar to the model eye alone (Figure 2). Since the lenslets in the peripheral lens do not share a common axis, but each directs rays toward the distant optic focus,[40] the standard sagittal power ("slope/r") calculation does not reveal the extra +3.50 D of add power in the lenslets (Figure 8a). However, when employing curvature power[46] (obtained from the wavefront using a discrete Laplacian calculation) the myopic defocus introduced by the lenslets can readily be seen (Figure 8b). However, the local curvature method is a noise-prone measure of optical power which generates spurious negative powers (up to −6 D) at the lenslet margins (dark blue ring of high negative power at the border of each lenslets, Figure 1c).[40] As a result, the defocus distributions obtained using the local curvature method show large amounts of myopic defocus at all TV, in line with the previously published reports of the effective myopia control nature of the lens.[10,18] The anomalous negative powers at the margins of the lenslets was reflected as artifactual hyperopic defocus (up to approximately 6 D) (Figure 8b) and highlights the complexity of correctly reporting power of a multi-segmented optical lens design.

Figure 9 shows the PSF and simulated retinal images of the "eye + DIMS" model with a minRMS focus of the distant optic while viewing through either the central or peripheral optics. As expected, the results of viewing through the central zone (with or without lag) are comparable to corresponding results of the model eye alone (minRMS focus). When viewing through the surround zone, the individually defocused PSF from the multiple lenslets superimposed on the PSF of the model eye (minRMS focus) generated low contrast images at 400 and 100 cm, but sufficient image quality to ensure legibility of the 16-point letter at near viewing distances (33 and 20 cm), both with and without the 0.50 D lag of accommodation (Figure 9c, d).

Model eye + NaturalVue Multifocal 1 Day lens

The NaturalVue Multifocal 1 Day lens is characterised by a smooth power profile over the central 6 mm pupil diameter

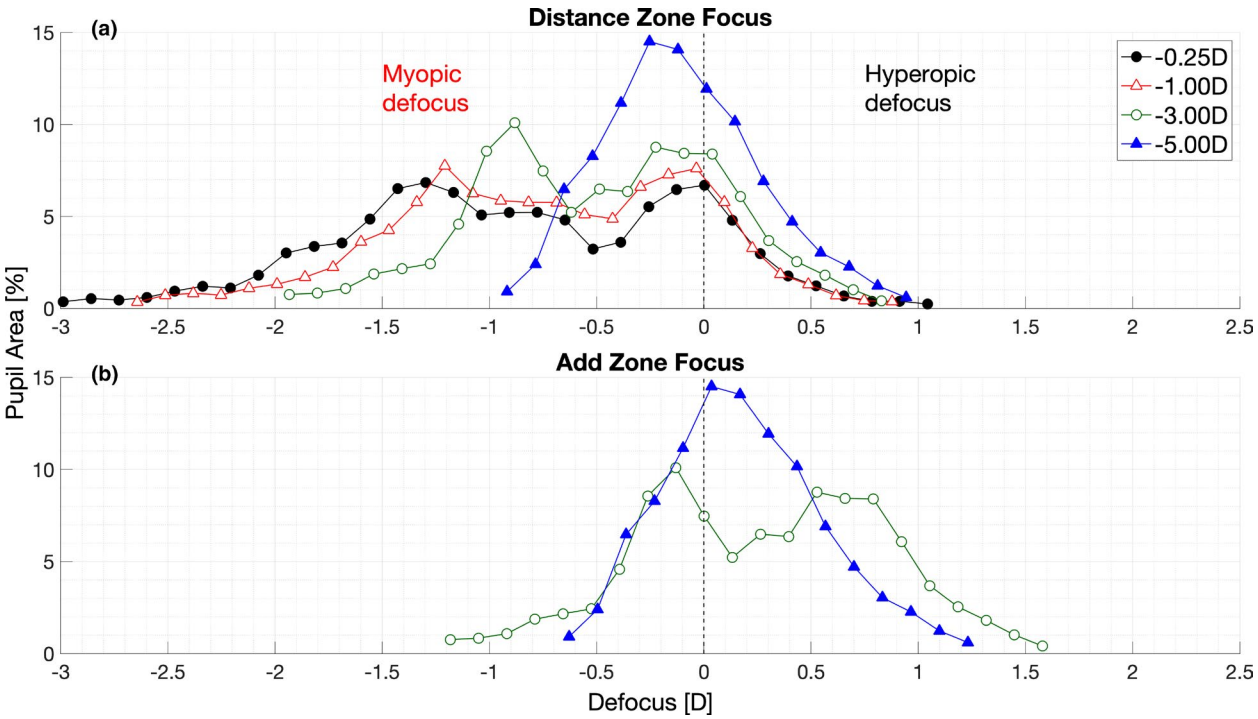

FIGURE 6 Impact of adding a Biofinity Multifocal centre-distance (CD) contact lens to the accommodating model child's eye. Defocus distributions using (a) distance focus at four different target vergences and (b) add zone focus (assuming +1.10 D add) at two near target vergences are shown. Defocus equals refractive state minus target vergence

due to highly aspheric optics. This power profile can be further characterised by a primary spherical aberration coefficient (C_4^0) of approximately +0.50 μm. The power of this design abruptly changes at a radius of around 3.0 mm such that the peripheral lens has a power closely matching the lens centre (Figure 1d). The defocus distributions for the "eye + NaturalVue" model are plotted in Figure 10 for the same four focusing strategies (minRMS, paraxial, optimum IQ, and marginal) as used for the model eye alone. However, unlike the eye alone, which generated a much wider defocus distribution at the closest viewing distance, the "eye + NaturalVue" model revealed wider distributions at the greater viewing distances (400, 100 and 33 cm). It also revealed a narrower defocus distribution at the 20 cm viewing distance, where: (a) the high negative SA of the model eye ($C_4^0 = -0.26$ μm) counteracted the positive SA of the lens (+0.42 μm) and (b) the pupil diameter was smaller than the lens aspheric zone. The positive SA of the lens remained dominant at greater distances, generating significant amounts of myopic defocus when optimally or paraxially focused. However, this positive SA reduced myopic defocus as the eye accommodated. Specifically, no significant myopic defocus was observed for the model "eye + lens" viewing at the closest distance of 20 cm. In contrast, the majority (>60%) of the defocus distributions at each TV were hyperopic with minRMS focus. The defocus distributions for the marginal focusing strategy which focused the edge of the centre optics or the maximum add region of the lens, resulted in the defocus distributions containing predominantly (>90%) hyperopic defocus at all TV (Figure 10d).

The PSF and simulated retinal images obtained for the "eye + NaturalVue" model (Figure 11) were similar when comparing each corresponding TV for both the paraxial and optimum IQ focusing strategies (Figure 11c–f), since optimum focus is close to paraxial focus for an eye with high levels of SA.[44] Image quality at 33 cm was most influenced by the focusing strategy and the accommodative lag. However, at a viewing distance of 20 cm, the legibility of the 16-point letter was retained for all focusing strategies, even in the presence of the added 0.50 D accommodative lag.

DISCUSSION

In this study, we used an optical model of an accommodating child's eye, in which both pupil size and the level of ocular SA changed with viewing distance, to assess the impact of multi-zone lenses on the legibility of 16-point type often encountered in children's literature.[27] Unlike the traditional use of multi-zone lenses with presbyopic eyes, in which the add power is used to aid focusing of near targets, multi-zone lenses in children aim to introduce myopic defocus in the retinal image of accommodating young eyes at all viewing distances.[47] In general, we found that all four lenses were able to successfully introduce significant myopic defocus without compromising legibility of 16-point type, even in the presence of plausible levels of accommodative lag (modelled with 0.50 D lag). There were, however, some exceptions to this general finding. The two

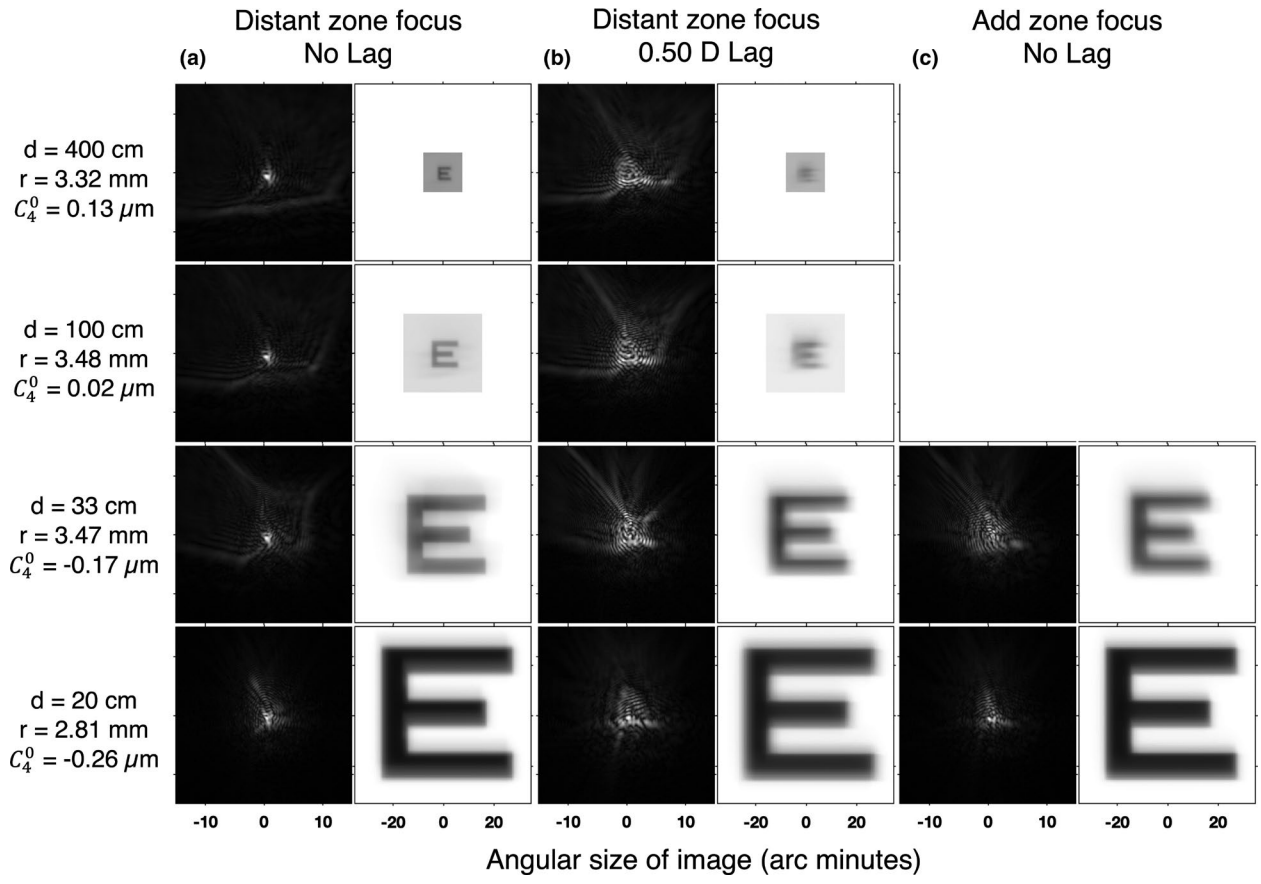

FIGURE 7 Impact of adding a Biofinity Multifocal centre-distance (CD) contact lens to the accommodating model child's eye. Point Spread Functions (PSF) and simulated retinal images of a letter E are computed for different viewing distances using distance zone focus and add zone focus as mentioned at the top. For distance zone focus, the effect of typical lag (0.50 D) is also shown

viewing-distance dependent changes of pupil diameter and ocular SA were responsible for removing the myopic defocus signal when viewing at near with the Biofinity Multifocal CD lens, in which the full near add was present for radii greater than 2 mm (excluding the transition zone). The amount of light entering the pupil after passing through the add zone was reduced from 64% (at 400 cm) to 49% (at 20 cm) due to pupil miosis. Also, the elevated levels of negative SA (−0.26 μm) present at the nearest viewing distance reduced the effective add for the "eye + Biofinity" model from about +1.40 D at 400 cm to <+0.25 D at 20 cm. The result of both pupil and SA changes converted the defocus distributions from the characteristic dual-focus, bi-modal distributions seen at 400 cm through 33 cm into an effectively monofocal distribution, lacking significant amounts of myopic defocus for the child viewing at 20 cm (Figure 6). A similar loss of multifocality and myopic defocus was also seen at 20 cm in the "eye + NaturalVue" model (Figure 10). In this case, the eye's negative SA simply cancelled out the lens' positive SA resulting in essentially a monofocal "eye + lens" combination. Loss of the myopic defocus signal essential to slow anomalous myopic eye growth suggests a potential low efficacy of these lenses in children who experience significant accommodative miosis and shifts toward higher levels of negative SA when viewing at near. This result may align with the variable myopia control responses clinically observed with multifocal lenses.[47]

Animal studies have shown that the presence of hyperopic defocus can be a "grow" signal, whereas myopic defocus is a "stop" signal for axial elongation in the young, developing eye,[48] and peripheral defocus may have a dominant influence on development of refractive error.[49] In an aberrated eye, only a portion of the light entering the pupil will be in focus, while the majority remains defocused. The effect of the relative strength of competing defocus signals is emphasised by Arumugam et al.,[50] who reported that even when the positively powered treatment zones occupied only one-fifth of the area of a dual-focus lens, refractive development in the treated monkeys was still dominated by relative myopic defocus. Even though different proportions (from 50:50 to 18:82) of +3.00 D/0.00 D zones were used in their lenses, the refractive errors (in all groups) were statistically similar to the monkeys reared with full field +3.00 D lenses. More recently, Walline et al.[51] reported that treatment with high add power, multi-zone lenses significantly reduced the rate of myopia progression compared to that of medium add powered lenses. This suggests that the magnitude rather than the proportion of myopic defocus may be crucial in controlling myopia

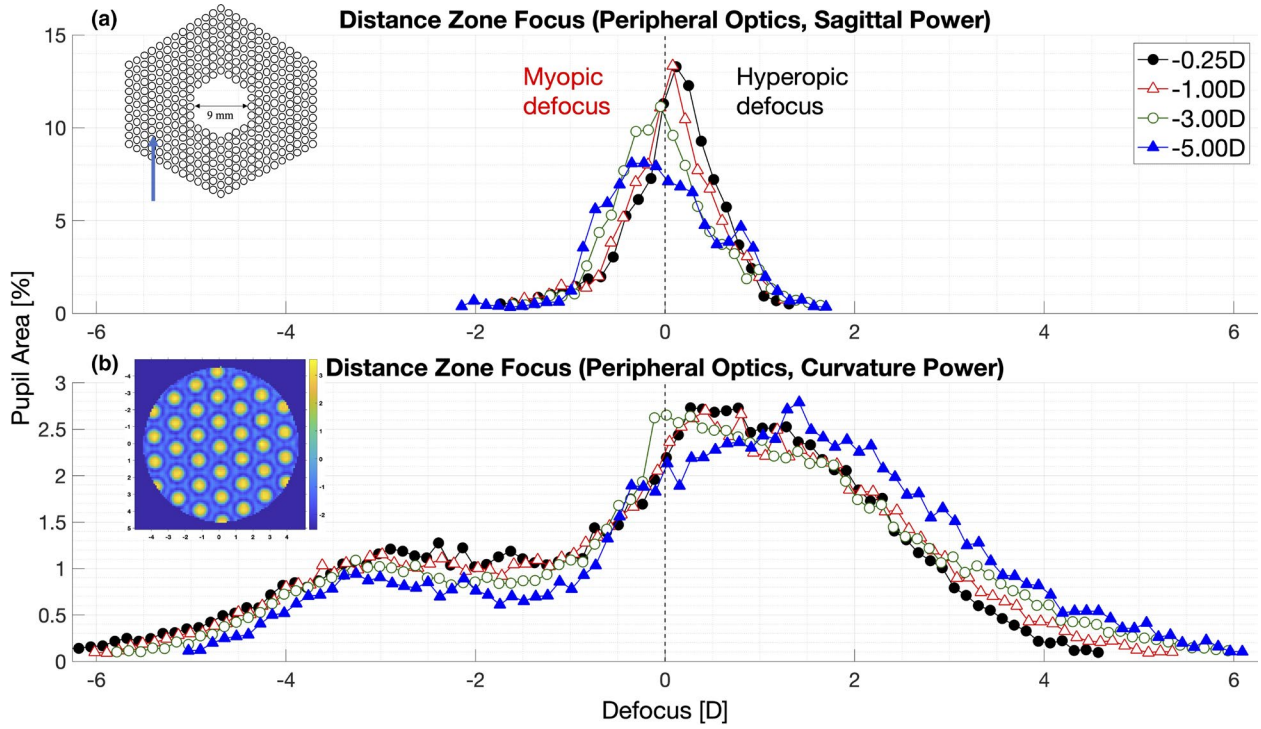

FIGURE 8 Impact of adding Defocus Incorporated Multiple Segments (DIMS) spectacle lens to the accommodating model child's eye. Defocus distributions at four different target vergences are shown for the model eye with minRMS focus of the distant optic and viewing through peripheral optics (assuming +3.50 D add), obtained by: (a) sagittal method and (b) local curvature method to compute power. The inset at the top (a) represents the geometry of the DIMS spectacle lens[40] with the arrowhead pointing to its peripheral optics, at the bottom (b) is the curvature power map of the peripheral optics. Note the different range of y-limits in (a) and (b) for better data visualization

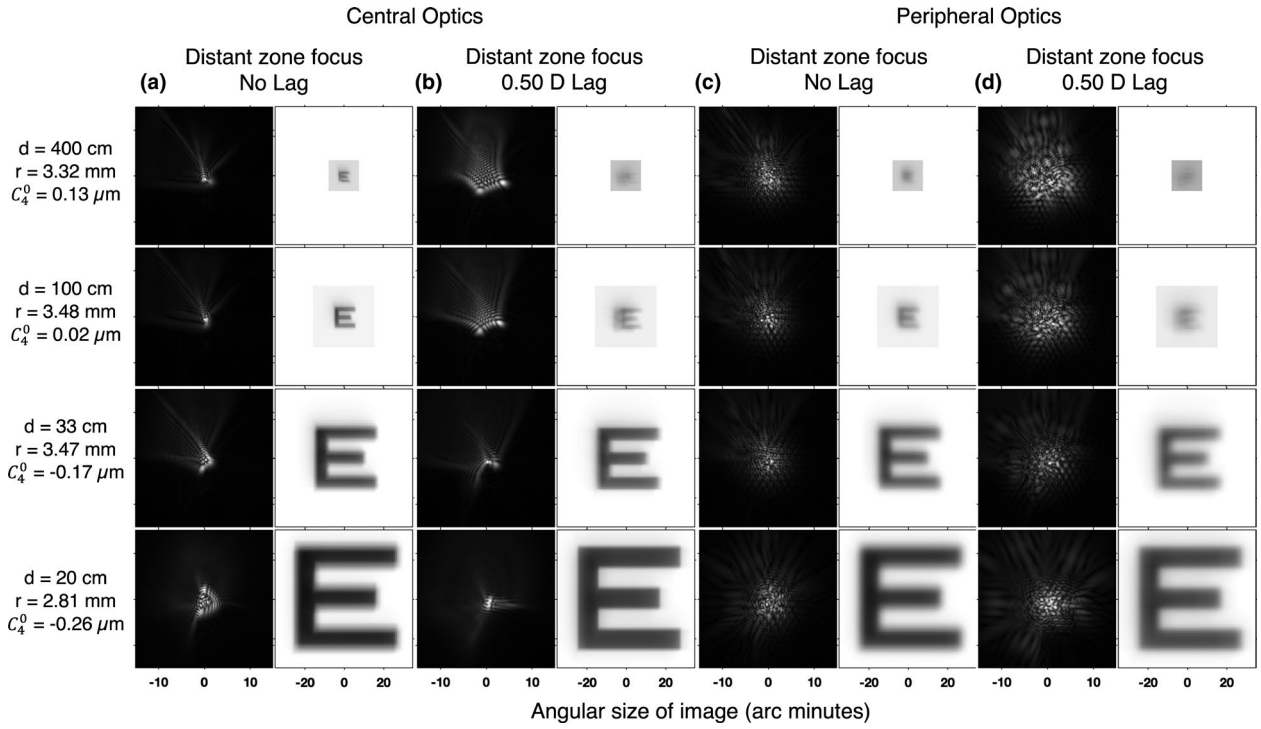

FIGURE 9 Impact of adding Defocus Incorporated Multiple Segments (DIMS) spectacle lens to the accommodating model child's eye. Point Spread Functions (PSF) and simulated retinal images of letter E are computed for the model eye with minRMS focus of the distant optic and viewing through either the (a, b) central or (c, d) peripheral optics, with and without the effect of typical lag (0.50 D) as mentioned at the top

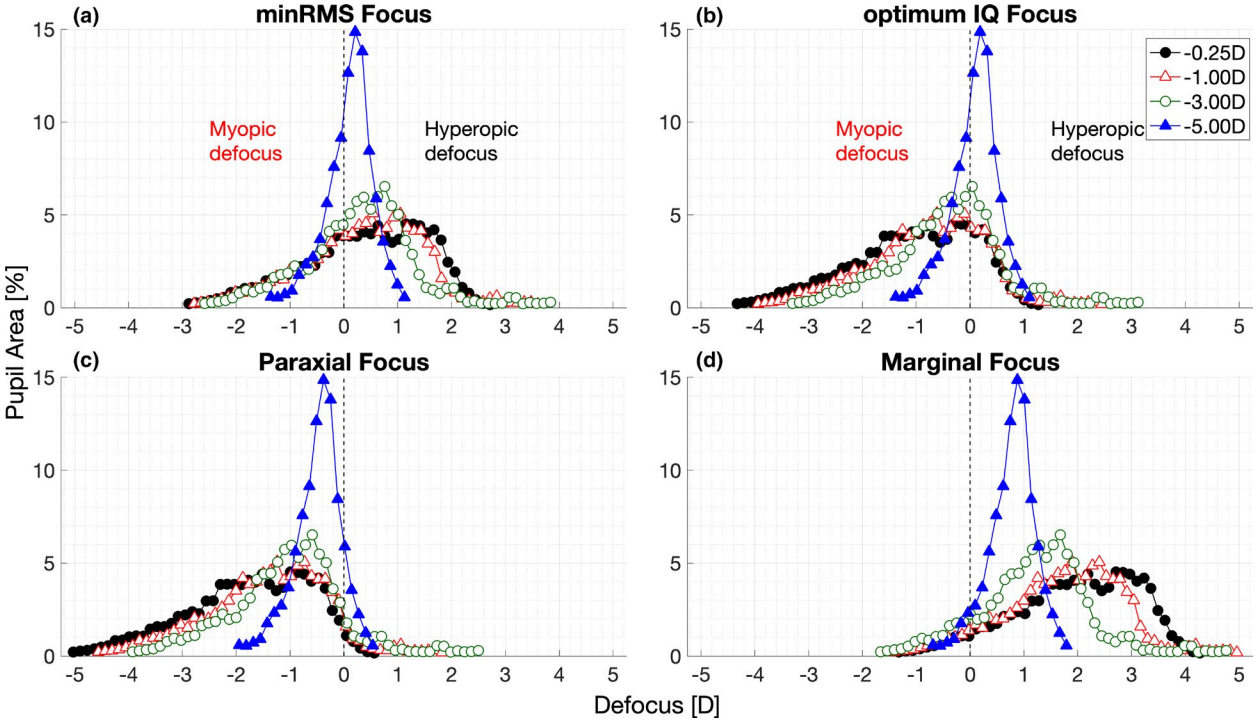

FIGURE 10 Impact of adding a NaturalVue Multifocal 1 Day contact lens to the accommodating model child's eye. Defocus distribution at four different target vergences employing different focusing strategies are shown. Defocus equals refractive state minus target vergence

progression. Our modelling results showed that although the "eye + Biofinity" model provided the maximum proportion of myopically defocused light at 400 cm (47% with >1.0 D of myopic defocus), myopic defocus exceeding 1.00 D was almost eliminated at the nearest viewing distance for both the "eye + Biofinity" and the "eye + NaturalVue" model. However, the "eye + MiSight" model sustained a significant level of myopic defocus at all viewing distances, (43% at 400 cm and about 30% each at 33 and 20 cm with >1.00 D of myopic defocus). The "eye + DIMS" model also generated significant levels of myopic defocus (40% at 400 cm and over 30% at 20 cm with >1.00 D of myopic defocus, ignoring defocus values >+2.00 D) (Figure 8b). Thus, even if the peripheral optics of the DIMS lens covered only half of the pupil (being a spectacle lens), it will still be able to produce 15% of myopic defocus >1.00 D at the closest viewing distance (20 cm).

The magnitudes of accommodative lag vary between children.[19] Typically they experience minimal to no lag when viewing distant targets, but lags tend to increase when viewing at near. Thus, for a typical child, a more reasonable model for retinal simulations would include no lag at 400 and 100 cm and with a typical lag (+0.50 D) at nearer viewing distances, such as 33 and 20 cm. Although the presence of aberrations (importantly negative SA) and blur from the accommodative lag degrade the image quality at near, this is typically compensated by the increased angular size of near targets[52] along with near viewing pupil miosis,[21] which expands the depth of field at near.[53] Considering a reasonable model, for the "eye alone" condition, the simulated retinal images yielded an easily legible text at all viewing distances almost irrespective of focusing approach (except marginal with no lag at 400 cm) (Figure 3).

Simulations of the model eye wearing MiSight 1 day or Biofinity Multifocal CD revealed legible text at near when either the distance or add zones were focused (Figures 5 and 7). However, as shown recently, both children[45] and young adults[22] fitted with MiSight lens accommodate to focus the distance optics. Interestingly, with Biofinity or NaturalVue lenses, increased accommodative lags were observed at near,[22] although they were generally less than the corresponding lens add powers. Because of the text legibility at near when either the distance or add zones were focused, children could focus with the add zones,[54] but the data clearly show for MiSight,[22,45] and perhaps also for Biofinity, that children and young adults do not adopt this accommodative strategy. Such behaviour may be absent because of the dominant impact of convergence on the accommodative response during binocular viewing.[55]

Although our optical model attempts to best represent a typical child's accommodating eye, several studies highlight the presence of significant individual variability in different optical parameters (e.g., SA, pupil diameter, accommodative lag, etc.) which can be further influenced by age, sex, race, refractive error, indoor/outdoor hours etc.[19–21,29,31,32,56] As our analysis shows, changes in these optical characteristics will affect the distributions of defocus and corresponding image quality, but likely will have little impact on the legibility of 16-point type at near. The current modelling analysis assumes complete contact lens conformation in agreement with previous results.[14,36] These earlier findings indicate that a lack of

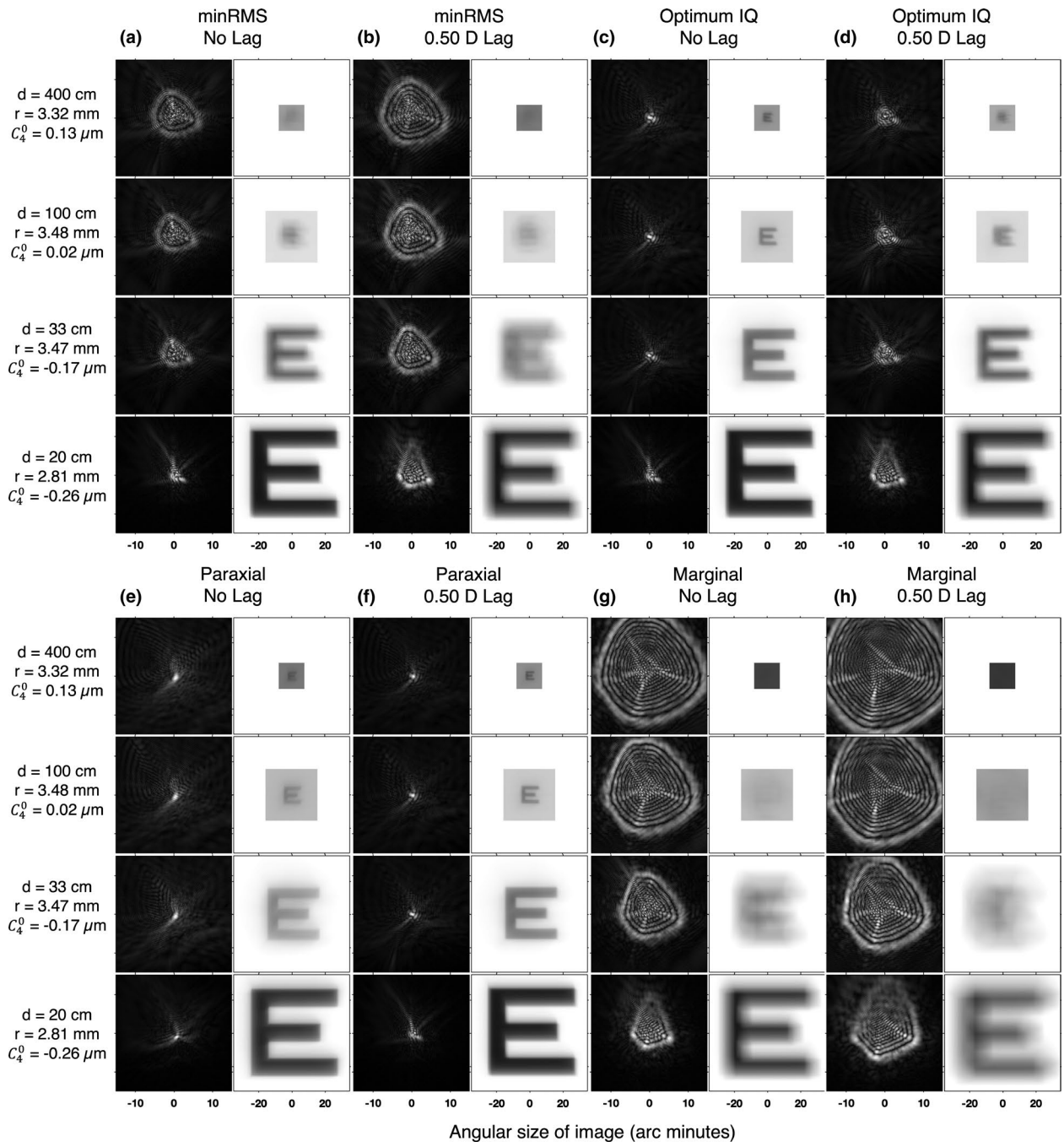

FIGURE 11 Impact of adding a NaturalVue Multifocal 1 Day contact lens to the accommodating model child's eye. Point Spread Functions (PSF) and simulated retinal images of a letter E computed for different viewing distances and employing different focusing strategies are shown at the top. For each refractive strategy, the effect of typical lag (0.50 D) is shown

conformity is not likely to occur for the on-axis conditions as modelled here, but may become more relevant in modelling certain off-axis conditions with high powered lenses.[14,36]

In summary, all four multi-zone lenses successfully generated myopic defocus at greater viewing distances, but two failed to introduce significant amounts of myopic defocus at the nearest viewing distance, when the model child's eye viewed through the central zone of the lens and used it to focus the target. Importantly, due to the magnification of the retinal image associated with near viewing, adding a multi-zone lens to a child's eye did not compromise legibility of a typical 16-point type character. Therefore, these lenses do not appear to impair reading ability of children when used as a myopia control tool.

ACKNOWLEDGMENTS

The authors thank Martin Rickert and Neeraj Singh for their help with the project.

CONFLICT OF INTEREST

None.

AUTHOR CONTRIBUTION

Raman Prasad Sah: Conceptualization (lead); Data curation (lead); Formal analysis (lead); Investigation (lead); Methodology (lead); Software (equal); Validation (equal); Visualization (equal); Writing – original draft (lead); Writing – review & editing (equal). **Matt Jaskulski:** Data curation (equal); Formal analysis (equal); Investigation (equal); Methodology (equal); Software (lead); Validation (equal); Visualization (equal); Writing – review & editing (equal). **Pete S Kollbaum:** Conceptualization (equal); Data curation (equal); Methodology (equal); Project administration (lead); Resources (equal); Software (equal); Supervision (lead); Validation (equal); Visualization (equal); Writing – review & editing (equal).

ORCID

Raman Prasad Sah https://orcid.org/0000-0003-4591-5012

REFERENCES

1. Vitale S, Ellwein L, Cotch MF, Ferris FL 3rd, Sperduto R. Prevalence of refractive error in the United States, 1999–2004. *Arch Ophthalmol* 2008;126:1111–9.
2. Chen M, Wu A, Zhang L, et al. The increasing prevalence of myopia and high myopia among high school students in Fenghua city, eastern China: a 15-year population-based survey. *BMC Ophthalmol* 2018;18:1–10. https://doi.org/10.1186/s12886-018-0829-8
3. Ding BY, Shih YF, Lin LLK, Hsiao CK, Wang IJ. Myopia among schoolchildren in East Asia and Singapore. *Surv Ophthalmol* 2017;62:677–97.
4. Jung SK, Lee JH, Kakizaki H, Jee D. Prevalence of myopia and its association with body stature and educational level in 19-year-old male conscripts in Seoul, South Korea. *Invest Ophthalmol Vis Sci* 2012;53:5579–83.
5. Wang TJ, Chiang TH, Wang TH, Lin LL, Shih YF. Changes of the ocular refraction among freshmen in National Taiwan University between 1988 and 2005. *Eye (Lond)* 2009;23:1168–9.
6. Gwiazda J, Hyman L, Hussein M, et al. A randomized clinical trial of progressive addition lenses versus single vision lenses on the progression of myopia in children. *Invest Ophthalmol Vis Sci* 2003;44:1492–500.
7. Walline JJ, Gaume Giannoni A, Sinnott LT, et al. A randomized trial of soft multifocal contact lenses for myopia control: Baseline Data and Methods. *Optom Vis Sci* 2017;94:856–66.
8. Chamberlain P, Peixoto-de-Matos SC, Logan NS, et al. A 3-year randomized clinical trial of MiSight lenses for myopia control. *Optom Vis Sci* 2019;96:556–67.
9. Bao J, Yang A, Huang Y, et al. One-year myopia control efficacy of spectacle lenses with aspherical lenslets. *Br J Ophthalmol* 2021;1–6. https://doi.org/10.1136/bjophthalmol-2020-318367 [online ahead of print].
10. Lam CS, Tang WC, Lee PH, et al. Myopia control effect of defocus incorporated multiple segments (DIMS) spectacle lens in Chinese children: results of a 3-year follow-up study. *Br J Ophthalmol* 2021;1–5. https://doi.org/10.1136/bjophthalmol-2020-317664
11. Dorronsoro C, Radhakrishnan A, de Gracia P, Sawides L, Marcos S. Perceived image quality with simulated segmented bifocal corrections. *Biomed Opt Express* 2016;7:4388–99.
12. Zheleznyak L, Kim MJ, MacRae S, Yoon G. Impact of corneal aberrations on through-focus image quality of presbyopia-correcting intraocular lenses using an adaptive optics bench system. *J Cataract Refract Surg* 2012;38:1724–33.
13. Kim MJ, Zheleznyak L, Macrae S, Tchah H, Yoon G. Objective evaluation of through-focus optical performance of presbyopia-correcting intraocular lenses using an optical bench system. *J Cataract Refract Surg* 2011;37:1305–12.
14. Kollbaum PS, Jansen ME, Tan J, Meyer DM, Rickert ME. Vision performance with a contact lens designed to slow myopia progression. *Optom Vis Sci* 2013;90:205–14.
15. Sha J, Tilia D, Diec J, et al. Visual performance of myopia control soft contact lenses in non-presbyopic myopes. *Clin Optom (Auckl)* 2018;10:75–86.
16. Gregory HR, Nti AN, Wolffsohn JS, Berntsen DA, Ritchey ER. Visual performance of center-distance multifocal contact lenses fit using a myopia control paradigm. *Optom Vis Sci* 2021;98:272–9.
17. Pomeda AR, Pérez-Sánchez B, Cañadas Suárez MDP, et al. MiSight Assessment Study Spain: A comparison of vision-related quality-of-life measures between MiSight contact lenses and single-vision spectacles. *Eye Contact Lens* 2018;44(Suppl 2):S99–S104.
18. Lam CSY, Tang WC, Tse DY, et al. Defocus Incorporated Multiple Segments (DIMS) spectacle lenses slow myopia progression: a 2-year randomised clinical trial. *Br J Ophthalmol* 2020;104:363–8.
19. Schmid KL, Strang NC. Differences in the accommodation stimulus response curves of adult myopes and emmetropes: a summary and update. *Ophthalmic Physiol Opt* 2015;35:613–21.
20. López-Gil N, Fernández-Sánchez V. The change of spherical aberration during accommodation and its effect on the accommodation response. *J Vis* 2010;10:12. https://doi.org/10.1167/10.13.12
21. Sah RP, Ramasubramanian V, Reed O, et al. Accommodative behavior, hyperopic defocus, and retinal image quality in children viewing electronic displays. *Optom Vis Sci* 2020;97:628–40.
22. Gifford KL, Schmid KL, Collins JM, et al. Multifocal contact lens design, not addition power, affects accommodation responses in young adult myopes. *Ophthalmic Physiol Opt* 2021;41:1346–54.
23. Kollbaum P, Jansen M, Thibos L, Bradley A. Validation of an off-eye contact lens Shack-Hartmann wavefront aberrometer. *Optom Vis Sci* 2008;85:E817–28.
24. Bao J, Chen H, Drobe B, Seow E, Lu F. Working distance during near work in emmetropic Chinese children. *Invest Ophthalmol Vis Sci* 2008;49:ARVO E-Abstract 1793.
25. Wang Y, Bao J, Ou L, Thorn F, Lu F. Reading behavior of emmetropic schoolchildren in China. *Vision Res* 2013;86:43–51.
26. Yeo AC, Atchison DA, Schmid KL. Children's accommodation during reading of Chinese and English texts. *Optom Vis Sci* 2013;90:156–63.
27. Burt C, Cooper WF, Martin JL. A psychological study of typography. *Br J Stat Psychol* 1955;8:29–56.
28. Legge GE, Bigelow CA. Does print size matter for reading? A review of findings from vision science and typography. *J Vis* 2011;11:1–22.
29. Kirwan C, O'Keefe M, Soeldner H. Higher-order aberrations in children. *Am J Ophthalmol* 2006;141:67–70.
30. Hughes RPJ, Read SA, Collins MJ, Vincent SJ. Higher order aberrations and retinal image quality during short-term accommodation in children. *Vision Res* 2021;188:74–84.
31. Subbaram MV, Bullimore MA. Visual acuity and the accuracy of the accommodative response. *Ophthalmic Physiol Opt* 2002;22:312–8.
32. Abbott ML, Schmid KL, Strang NC. Differences in the accommodation stimulus response curves of adult myopes and emmetropes. *Ophthalmic Physiol Opt* 1998;18:13–20.
33. Lam CSY, Tang WC, Qi H, et al. Effect of Defocus Incorporated Multiple Segments spectacle lens wear on visual function in myopic Chinese children. *Transl Vis Sci Technol* 2020;9:1–10. https://doi.org/10.1167/tvst.9.9.11
34. Cooper J, O'Connor B, Watanabe R, et al. Case series analysis of myopic progression control with a unique extended depth of focus multifocal contact lens. *Eye Contact Lens* 2018;44:e16–24.
35. U.S. Food and Drug Administration. MiSight 1 day (omafilcon A) soft (hydrophilic) contact lenses for daily wear - P180035 | FDA.

Available from: https://www.fda.gov/medical-devices/recently-approved-devices/misight-1-day-omafilcon-soft-hydrophilic-contact-lenses-daily-wear-p180035 Accessed 24 Aug 2021.
36. Jaisankar D, Liu Y, Kollbaum P, et al. Nasal-temporal asymmetry in peripheral refraction with an aspheric myopia control contact lens. *Biomed Opt Express* 2020;11:7376–94.
37. Thibos LN, Hong X, Bradley A, Applegate RA. Accuracy and precision of objective refraction from wavefront aberrations. *J Vis* 2004;4:329–51.
38. Thibos LN, Bradley A, López-Gil N. Modelling the impact of spherical aberration on accommodation. *Ophthalmic Physiol Opt* 2013;33:482–96.
39. Altoaimi BH, Almutairi MS, Kollbaum PS, Bradley A. Accommodative behavior of young eyes wearing multifocal contact lenses. *Optom Vis Sci* 2018;95:416–27.
40. Jaskulski M, Singh NK, Bradley A, Kollbaum PS. Optical and imaging properties of a novel multi-segment spectacle lens designed to slow myopia progression. *Ophthalmic Physiol Opt* 2020;40:549–56.
41. Atchison DA, Joblin A, Smith G. Influence of Stiles-Crawford effect apodization on spatial visual performance. *J Opt Soc Am A* 1998;15:2545–51.
42. Atchison DA, Scott DH, Strang NC, Artal P. Influence of Stiles-Crawford apodization on visual acuity. *J Opt Soc Am A* 2002;19:1073–83.
43. Legras R, Chateau N, Charman WN. A method for simulation of foveal vision during wear of corrective lenses. *Optom Vis Sci* 2004;81:729–38.
44. Xu R, Bradley A, Thibos LN. Impact of primary spherical aberration, spatial frequency and Stiles Crawford apodization on wavefront determined refractive error: a computational study. *Ophthalmic Physiol Opt* 2013;33:444–55.
45. Ruiz-Pomeda A, Perez-Sanchez B, Canadas P, et al. Binocular and accommodative function in the controlled randomized clinical trial MiSight(R) Assessment Study Spain (MASS). *Graefes Arch Clin Exp Ophthalmol* 2019;257:207–15.
46. Thibos LN, Hong X, Bradley A, Applegate RA. Metrics of optical quality of the eye. *J Vis* 2003;4:1–15.
47. Walline JJ, Greiner KL, McVey ME, Jones-Jordan LA. Multifocal contact lens myopia control. *Optom Vis Sci* 2013;90:1207–14.
48. Arumugam B, Hung LF, To CH, Holden B, Smith EL 3rd. The effects of simultaneous dual focus lenses on refractive development in infant monkeys. *Invest Ophthalmol Vis Sci* 2014;55:7423–32.
49. Smith EL 3rd. Prentice Award Lecture 2010: A case for peripheral optical treatment strategies for myopia. *Optom Vis Sci* 2011;88:1029–44.
50. Arumugam B, Hung LF, To CH, Sankaridurg P, Smith EL III. The effects of the relative strength of simultaneous competing defocus signals on emmetropization in infant rhesus monkeys. *Invest Ophthalmol Vis Sci* 2016;57:3949–60.
51. Walline JJ, Walker MK, Mutti DO, et al. Effect of high add power, medium add power, or single-vision contact lenses on myopia progression in children: The BLINK randomized clinical trial. *JAMA* 2020;324:571–80.
52. Xu R, Chelales E, Rickert M, et al. Small text on product labels poses a special challenge for emerging presbyopes. *Optom Vis Sci* 2019;96:291–300.
53. Charman WN. Pinholes and presbyopia: solution or sideshow? *Ophthalmic Physiol Opt* 2019;39:1–10.
54. Faria-Ribeiro M, Amorim-de-Sousa A, Gonzalez-Meijome JM. Predicted accommodative response from image quality in young eyes fitted with different dual-focus designs. *Ophthalmic Physiol Opt* 2018;38:309–16.
55. Fincham EF, Walton J. The reciprocal actions of accommodation and convergence. *J Physiol* 1957;137:488–508.
56. Plainis S, Ginis HS, Pallikaris A. The effect of ocular aberrations on steady-state errors of accommodative response. *J Vis* 2005;5:466–77.

SUPPORTING INFORMATION

Additional supporting information may be found in the online version of the article at the publisher's website.

How to cite this article: Sah RP, Jaskulski M, Kollbaum PS. Modelling the refractive and imaging impact of multi-zone lenses utilised for myopia control in children's eyes. *Ophthalmic Physiol Opt* 2022;42:571–585. https://doi.org/10.1111/opo.12959